



NSF Projects: CNS-1645863 & CMMI-1100742

Drive-by and Fly-by Bridge Monitoring and Damage Detection Technology

Prof. Nasim Uddin, PE, F.ASCE (PI)

(Editor-in-Chief of ASCE Natural Hazards Review Journal)

(Drs. M. Yahya, M. Elhatab, C. Tan, S. Polydorou

Prof. M. Haider (UAB), E. O'Brien, A. Gonzalez (UCD), S. Taylor (QUB))

Civil, Construction, and Environmental Engineering
University of Alabama at Birmingham

Problems

- (1) Current management methods are reliant on visual inspections which only provide qualitative information and introduce subjectivity
- (2) Due to continuous monitoring, extremely large volume of data accumulates in a short period of time, e.g., a single sensor channel sampled at 200 Hz generates 34 MB of data in one day or 12.6 GB of data in one year. Already have a burden of large inventory of structures requiring structural health monitoring (SHM) technologies.
- (3) Requirement of a continuous power supply on every bridge in the network. Constitutes a prohibitive cost for every bridge in the stock.
- (4) The causal relationship between repeated truck loading and long-term structural deterioration is not well understood. Current SHM systems are only telling half of the story. The solution to the bridge safety problem is, therefore, two-fold: control of overloaded trucks, and safety assessment/monitoring of bridges and their loads.

SHM Systems are not portable, it cannot be moved easily from one bridge to another, the cost accompanied with that makes the systems dramatically expensive.





Few major bottlenecks currently exist that severely limit the effectiveness of existing bridge health management methods.

Continuous power supply



Extremely large volume of data



Understand the relationship between loading and structural deterioration





*Few major
bottlenecks
currently exist
that severely limit
the effectiveness
of existing bridge
health
management
methods.*

*Continuous
power supply*



*Extremely large
volume of data*



*Understand the relationship
between loading and
structural deterioration*





Investigation of damage detection and Load Control algorithms by “short data burst”

- The use of *limited number of sensor channels*, will lead to **shorter length of data streams** than that of the conventional SHM.
- Bridge vibrations induced by everyday traffic and environmental loading are collected by SHM systems to capture features of the bridge (e.g., frequencies and mode shapes).
- **Mode shapes in particular have great potential to identify, locate and quantify deterioration** but have not been successfully used to date because (i) **many sensors are required** and (ii) **robust post-processing** methods do not exist that can successfully extract mode shapes from measured accelerations.

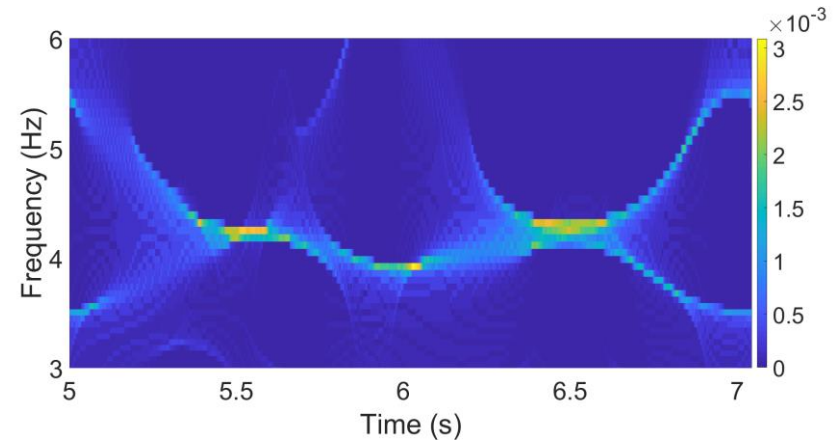
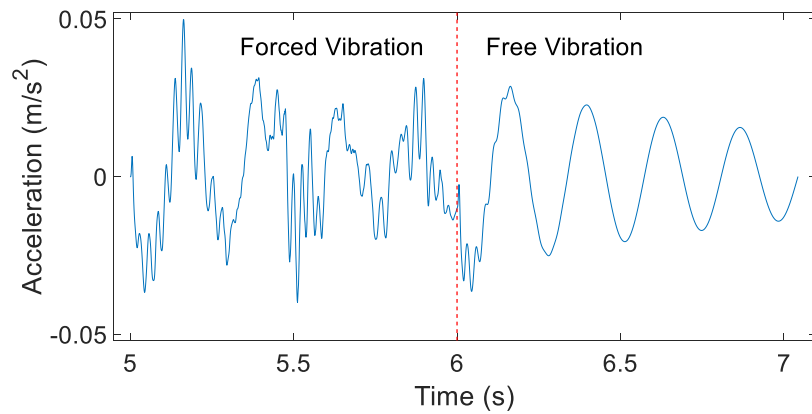


2 - Extremely large volume of data problem

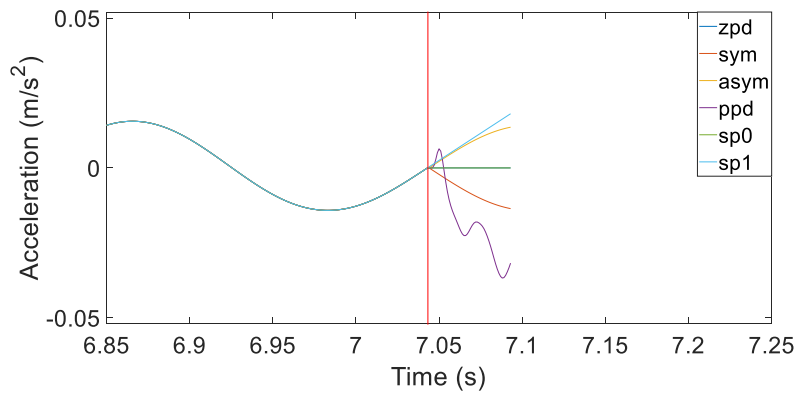
- To overcome this problem new type of damage detection algorithms have been developed called

“Short Data Burst”.

- This type of algorithms deal with signals less than 5 sec.



Short data burst (left) and frequency spectrum by SWT (right).



- 1) Zero Padding (zpd).
- 2) Symmetry Padding (sym).
- 3) Anti-Symmetry Padding (asym).
- 4) Periodic Padding (ppd).
- 5) Smooth of Order 0 Padding (sp0).
- 6) Smooth of Order 1 Padding (sp1).

Examples of signal extension.



PADDING TECHNIQUE	Noise-free	SNR		
		50	20	5
original	0.4365	0.4360	0.4383	0.4373
zpd	0.1682	0.1683	0.1664	0.1693
sym	0.3008	0.3058	0.3058	0.3058
asym	0.1692	0.1697	0.1689	0.1711
ppd	0.3904	0.3904	0.3904	0.3904
sp0	0.1682	0.1683	0.1668	0.1694
sp1	0.1680	0.1693	0.1845	0.1857

RMSE (Hz) for different padding techniques and noise levels.



Conclusion & Future Plan ---- Part 1:

- 1) The results have highlighted that all padding techniques under investigation have rendered better estimation of frequencies than not applying padding at all. In the case of a noise-free signal, **symmetry padding and periodic padding perform worse than the others**. Based on the RMSE, smooth padding of order 1 and 0, **zero padding, and anti-symmetry padding** have clearly outperformed symmetry and periodic types of padding.
- 1) Further research aims to propose an efficient technique able to deal with the discontinuity at the transition period between forced and free vibration.



*Few major
bottlenecks
currently exist
that severely limit
the effectiveness
of existing bridge
health
management
methods.*

*Continuous
power supply*



*Extremely large
volume of data*

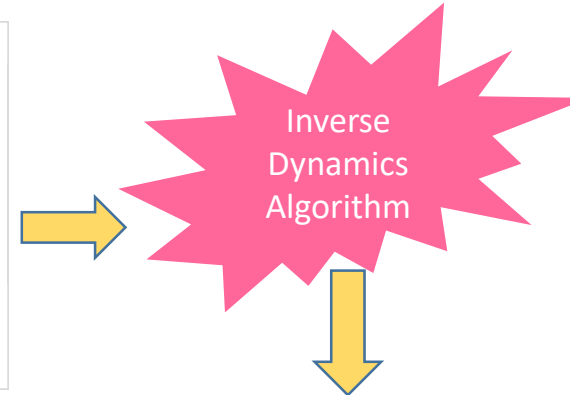
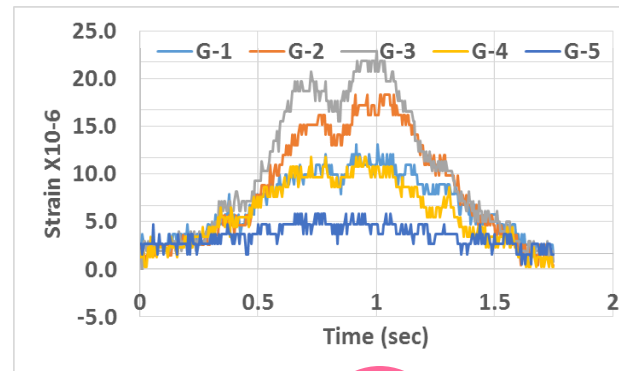
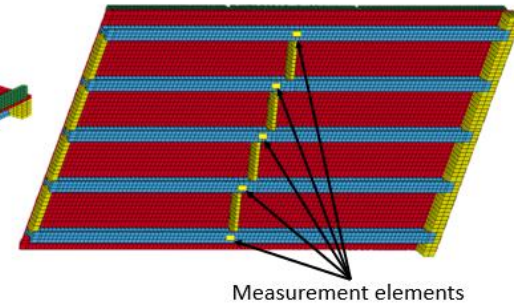
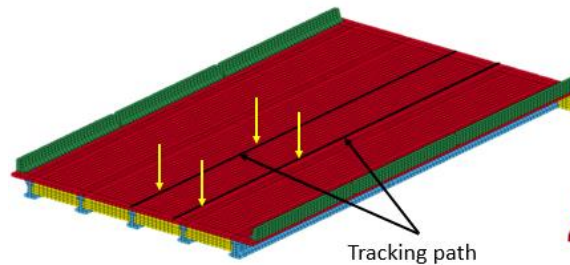


*Understand the relationship
between loading and
structural deterioration*

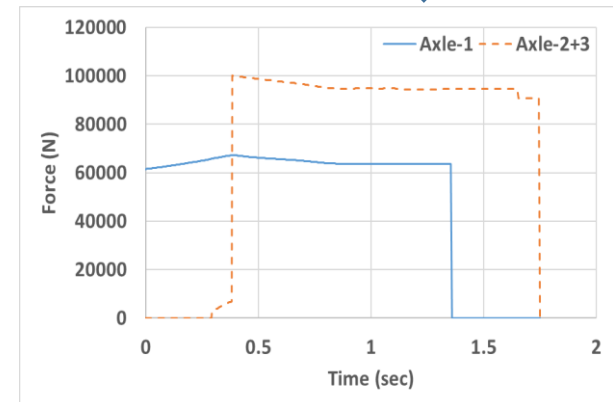




3a - Load Control (B-WIM SYSTEM)

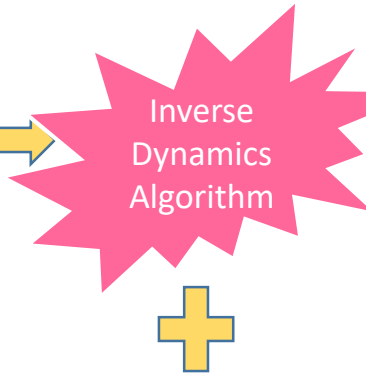
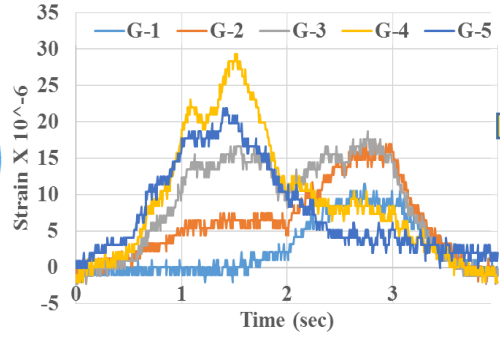


Item	Static weight	Calculated weight	Error (%)
Axle-1	66700	65046	-2.54
Axles 2+3	94800	95005	+0.22
GVW	161500	160051	-0.90



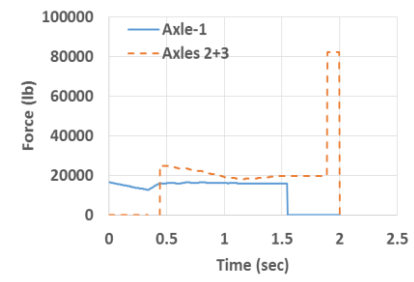


3b- Load Control (Multiple-Presence)

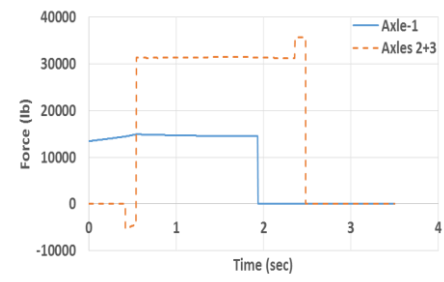


Item	Static weight (lb.)	Calculated weight (lb.)	Error (%)
Axle-1	15100	15866	5.07
Axles 2+3	21300	19278	-9.49
GVW	36400	35145	-3.44

Item	Static weight (lb.)	Calculated weight (lb.)	Error (%)
Axle-1	16150	14689	9.04
Axles 2+3	29050	31420	-8.16
GVW	45200	46110	-2.01



Second Truck Force History



First Truck Force History





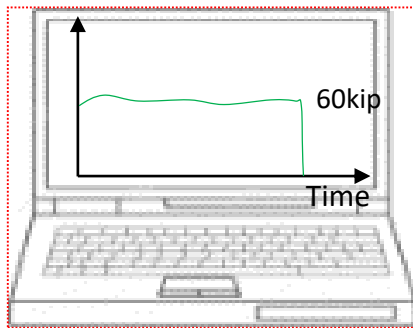
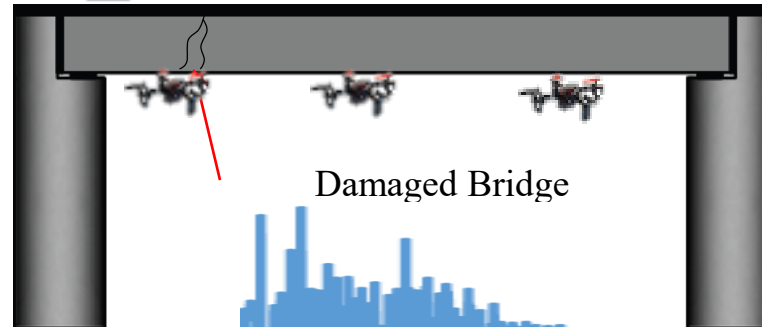
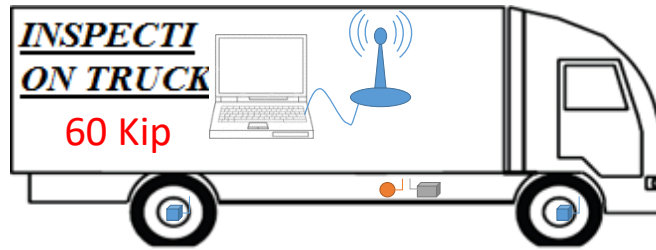
Challenges facing current B-WIM system and all SHM systems

- **Installation Time**
- **Complexity**
- **Access to bridges underneath**
- **Cost**

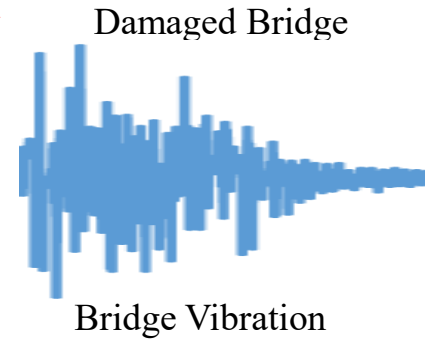




4 - Drone Sensors

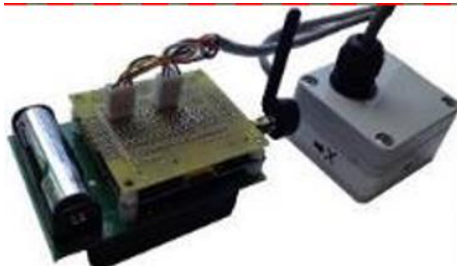


Truck weight



Drone Accelerometers

- The benefits of switching to this is unprecedented.
- **But why this has not been used to date ????**
- Bridge Vibration is of small amplitude in which requiring a very sensitive sensors to record this vibration.



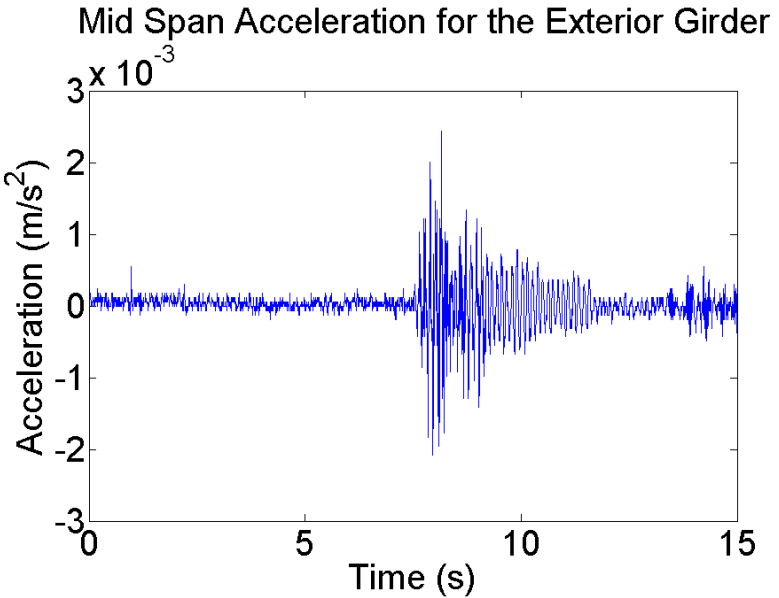
Silicon Designs 2012-002 accelerometers
Detect signal with power of 1⁻⁴ dB



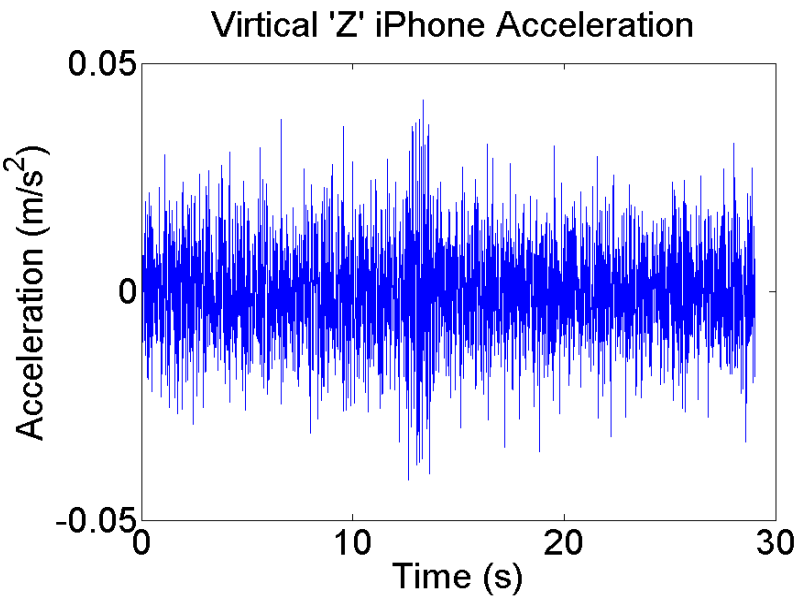
iPhone has M9 accelerometer Designed for Tracking the human activities
Detect signal with power of 10 dB

Drone Accelerometers

- So if off-the-shelf devices used to record the bridge vibration, the vibration will totally disrupted by the noise



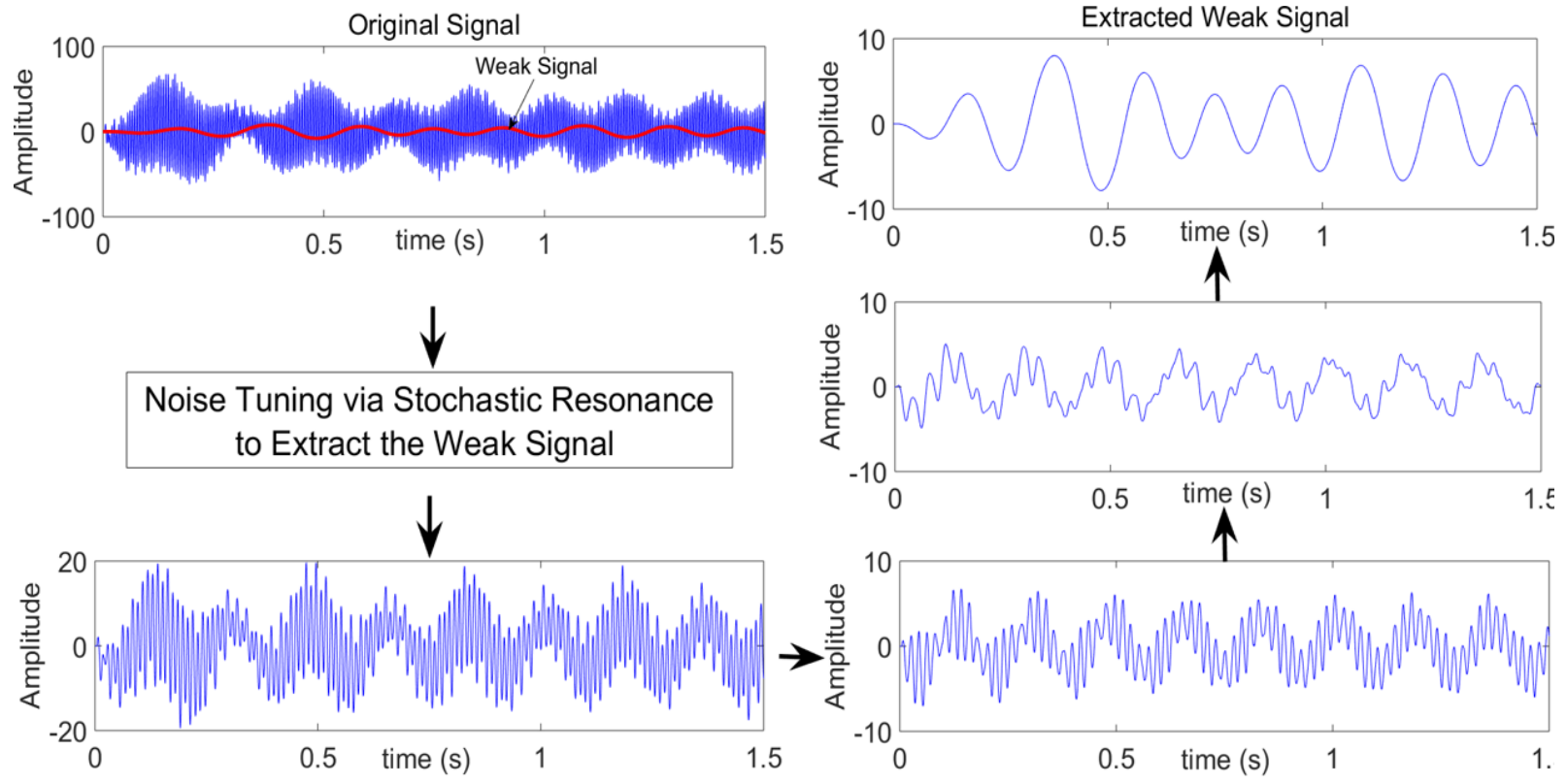
Silicon Designs Record for bridge vibration



iPhone Record for bridge Vibration

Introduction to Stochastic Resonance

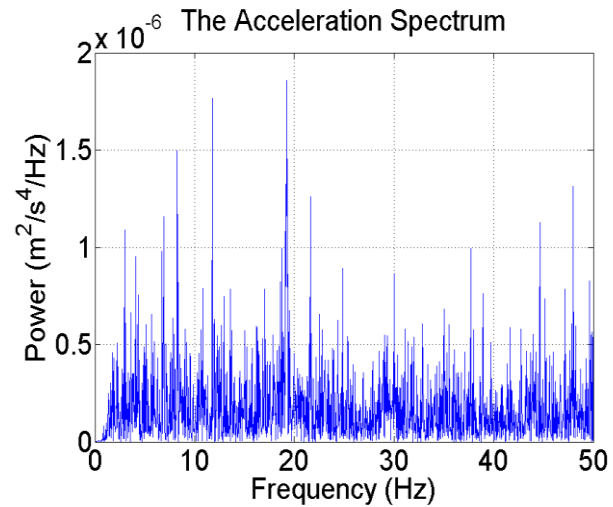
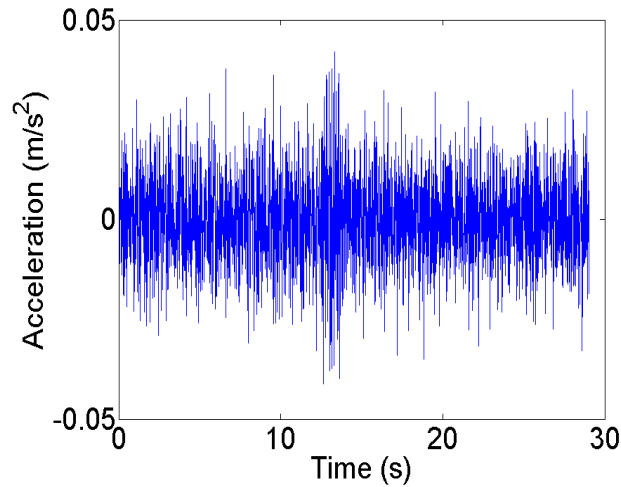
- This example demonstrate the application of conventional SR



Stochastic Resonance: Extract Bridge Frequency Using iPhone acceleration.

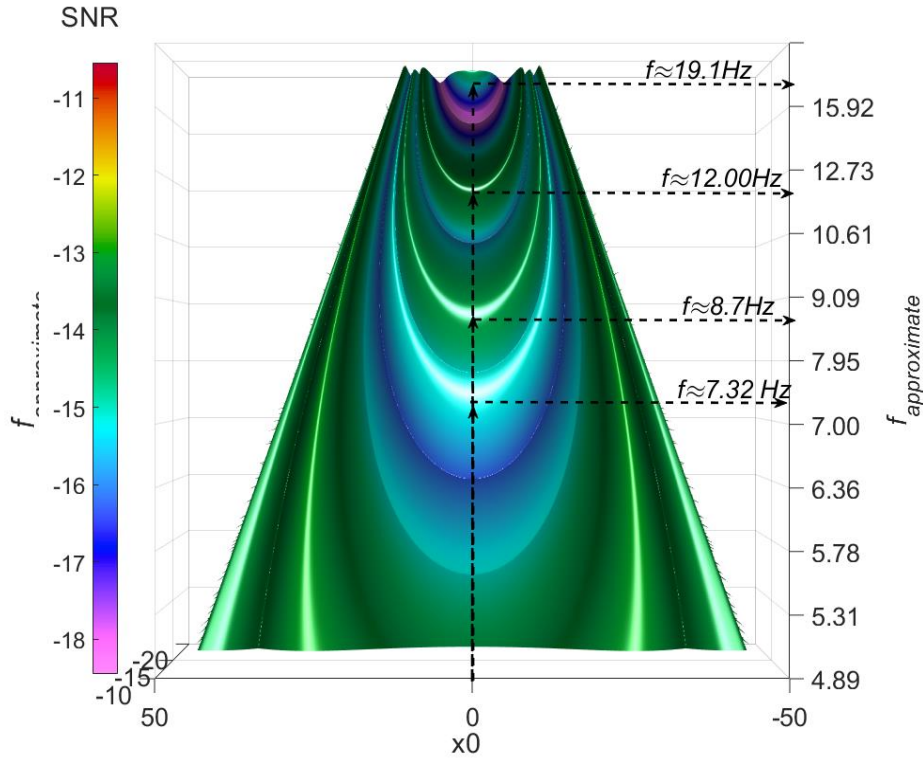
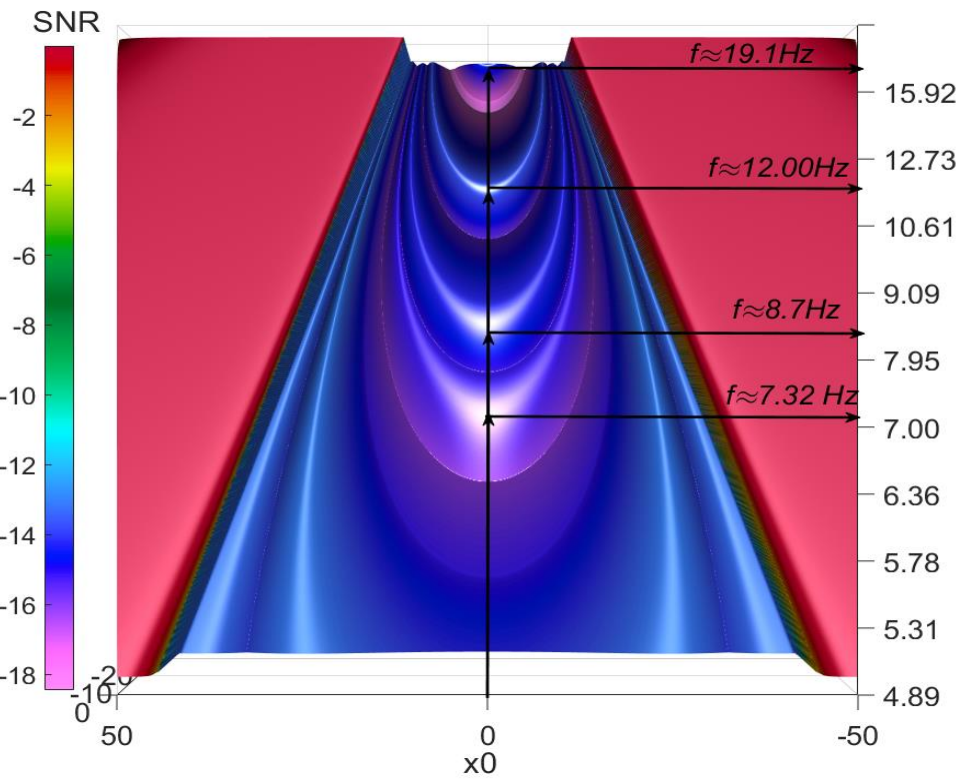


Vertical 'Z' iPhone Acceleration



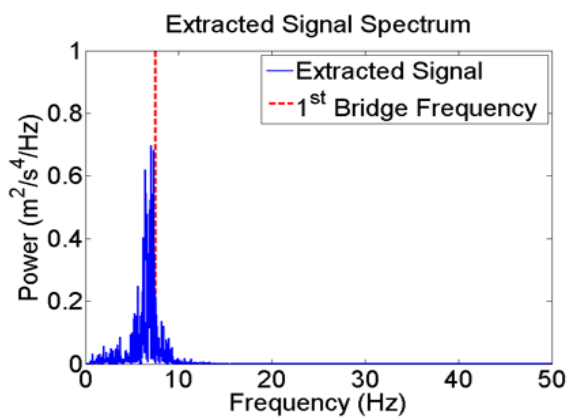
Extracting Bridge Frequency using an iPhone

- SR results was very promising.

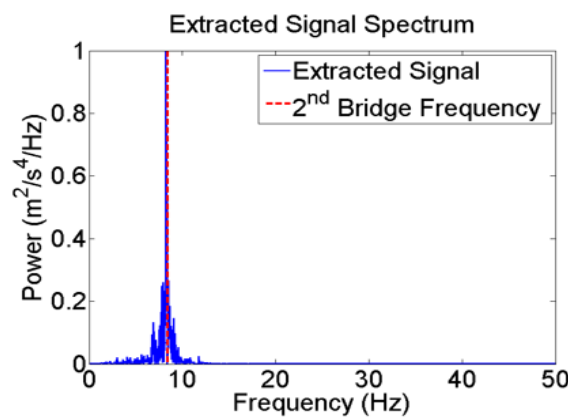


Extracting Bridge Frequency using an iPhone

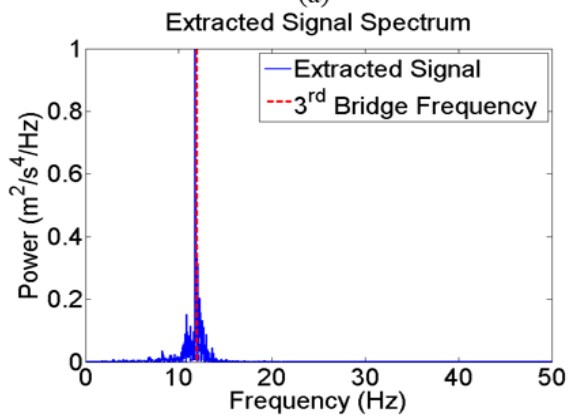
- The algorithm Successfully identifies the first four bridge frequencies.



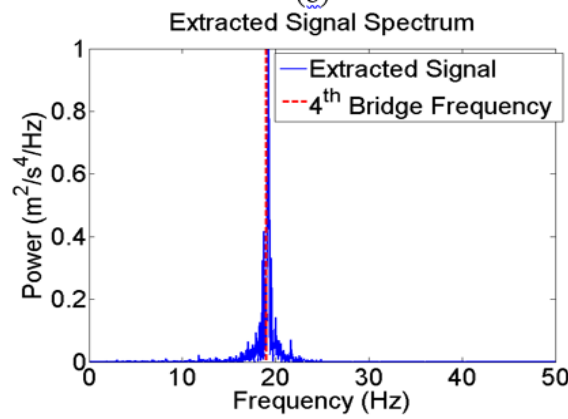
(a)



(b)



(c)



(d)

Flying Sensor

Accelerometer will be install inside the drone which equipped by perching mechanism allows drone to stick to any steel structure



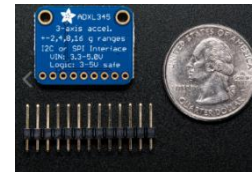
Electromagnet

Receiver Working Voltage Input DC3.5V-12V



Your Load (LED,Button etc) Working Voltage DC1V-24V

Mini relay wireless switch



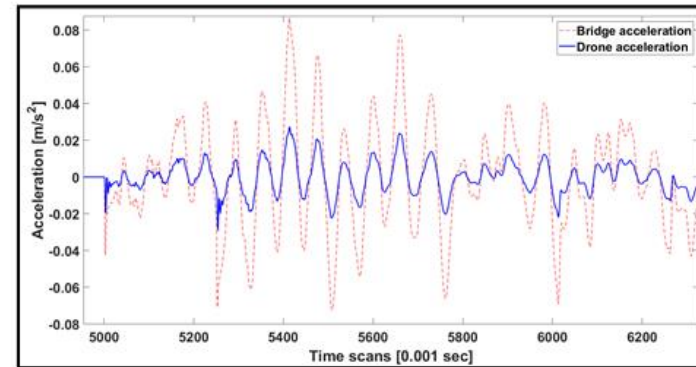
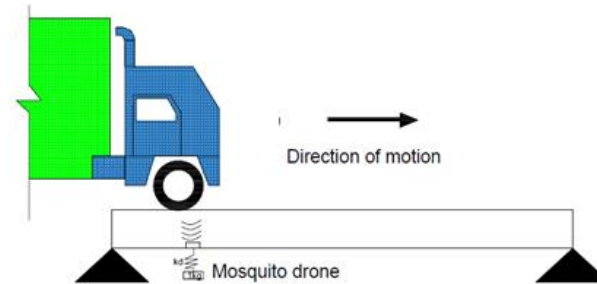
Accelerometer



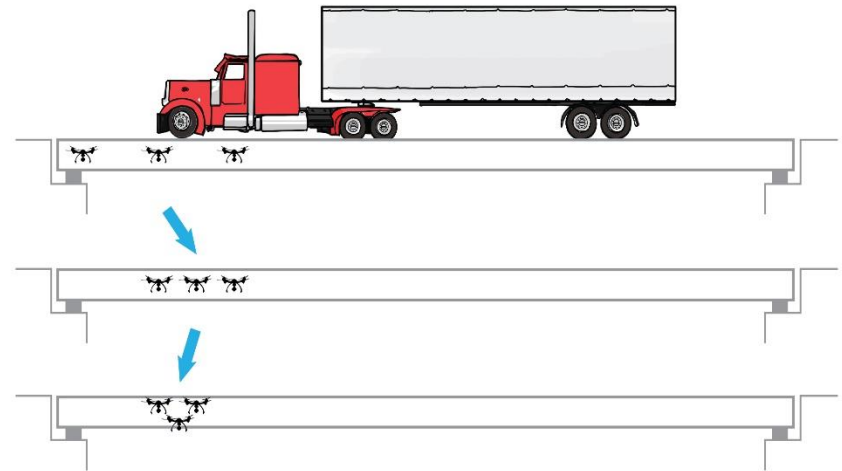
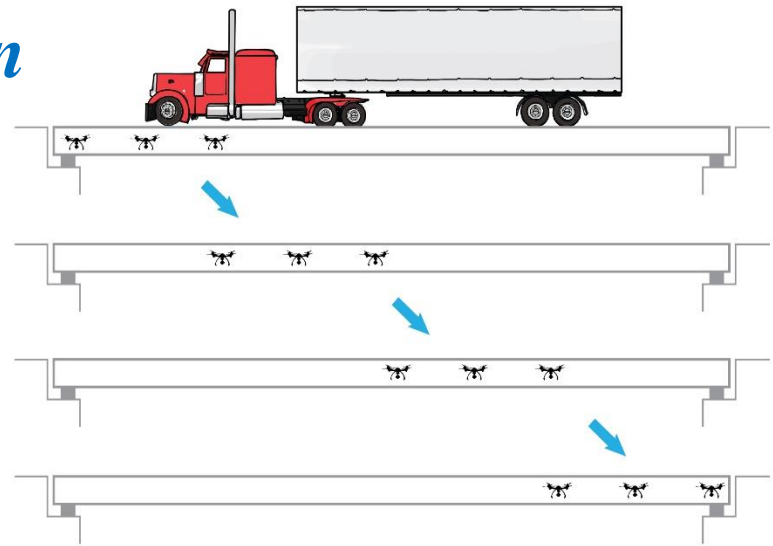
Drone



Flying Sensor



7 – Drone Flock Orchestration



8 - Damage Detection from Image (detailed image of damage and actual location)



- To detect small cracks drone should fly close enough to detect it.



- But it will be hard to know where is this crack in the whole bridge.





Crack Detection using Faster R-CNN and Point Feature Matching



a) Drone with camera
(UAB lab)



b) Drone hovering



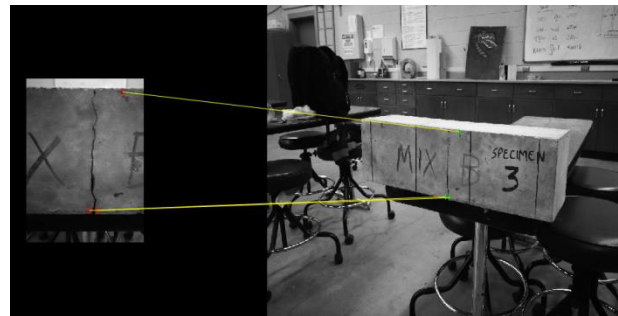
c) Inspected beam
(Target image)



Crack photo



Beam photo



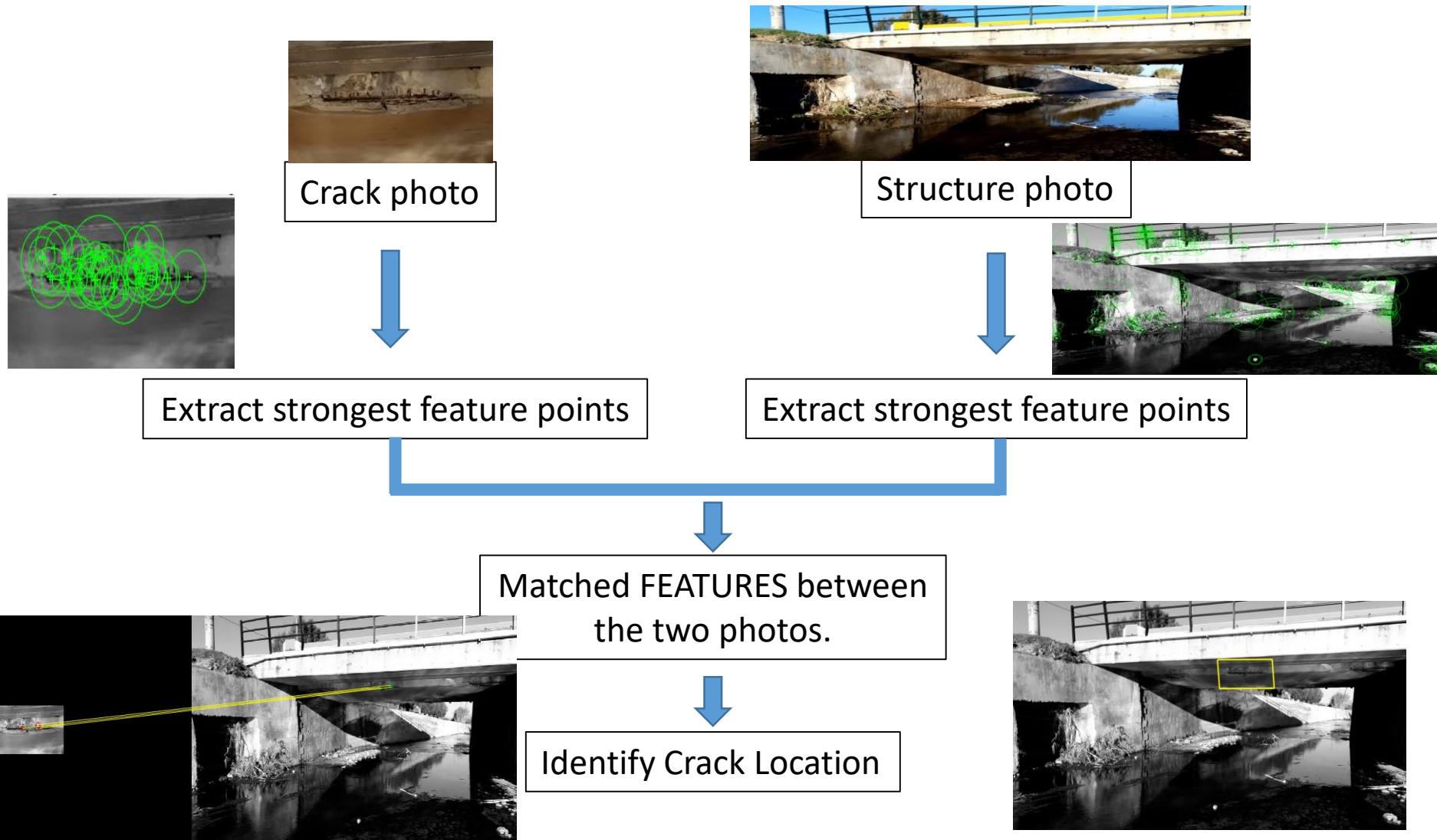
Matched FEATURES between
the two photos.



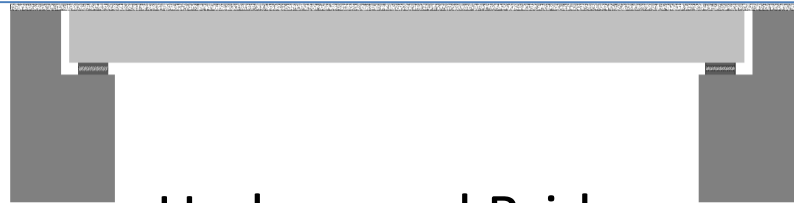
Crack Location



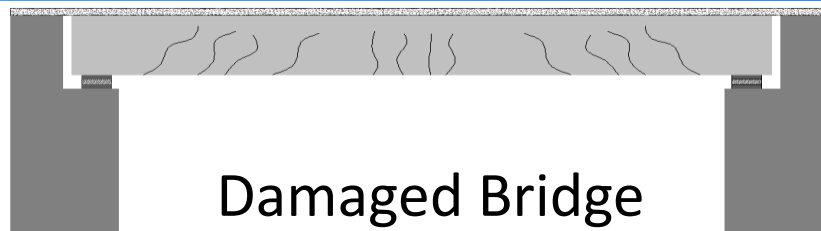
- We solved this challenge using Point Feature Matching algorithm



➤ 9 - Drive-By Bridge Inspection



Undamaged Bridge



Damaged Bridge



*Few major
bottlenecks
currently exist
that severely limit
the effectiveness
of existing bridge
health
management
methods.*

*Continuous
power supply*



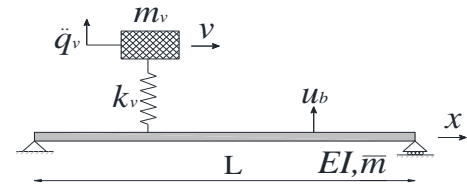
*Extremely large
volume of data*



*Understand the
relationship between
loading and structural
deterioration*



How 'drive-by' bridge inspection works?



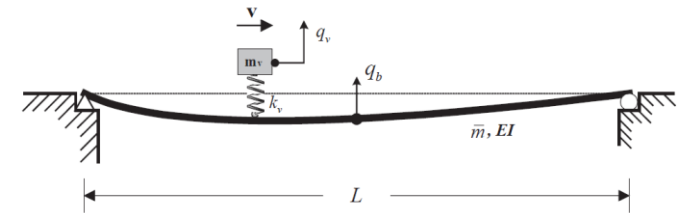
The conception of “drive-by” is first developed by Y.B. Yang etc. [1].

Bridge motion equation: $\bar{m}\ddot{u} + EIu'''' = f_c(t)\delta(x - vt)$

Vehicle motion equation: $m_v\ddot{u} + k_v(q_v - u|_{x=vt}) = 0$

$$\ddot{q}_v(t) = \sum_{n=1}^{\infty} \left\{ \begin{array}{l} \bar{A}_{1,n} \cos\left(\frac{(n-1)\pi v}{L}t\right) + \bar{A}_{2,n} \cos\left(\frac{(n+1)\pi v}{L}t\right) + \bar{A}_{3,n} \cos(\omega_v t) \\ + \bar{A}_{4,n} \cos\left(\omega_{b,n} - \frac{n\pi v}{L}t\right) + \bar{A}_{5,n} \cos\left(\omega_{b,n} + \frac{n\pi v}{L}t\right) \end{array} \right\}$$

Vehicle and bridge interaction



- The vehicle response contains vibration components dominated by the natural frequencies of bridge

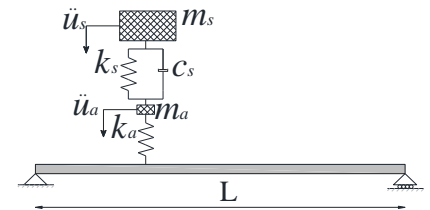


Drive-by bridge SHM

- The natural bridge frequencies
- The bridge damping
- The mode shapes
- To detect the discontinuity with signal processing tool as wavelet transform & Hilbert transform, etc.

- Bridge frequencies

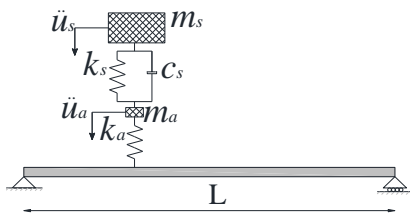
- FFT
- The limited Vehicle and Bridge Interaction time
- **low resolution** of FFT spectrum
- It cannot detect the frequency drop caused by damages



Using the **pseudo-frequency** of wavelet transform to replace FFT

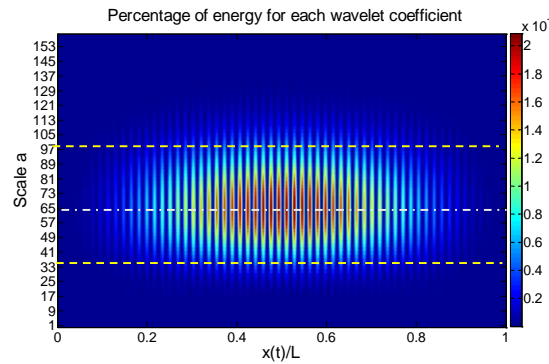
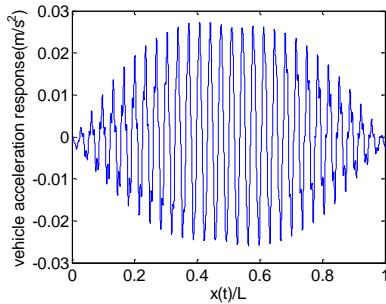
• Wavelet Theory

- FT only works as a **signal-converting tool** from the time domain to the frequency domain.
- While, performing wavelet transforms, a **signal is shown in the frequency domain while the information in the time domain still retained**.
- Wavelet analysis gives better **frequency-time information** to objective signals.

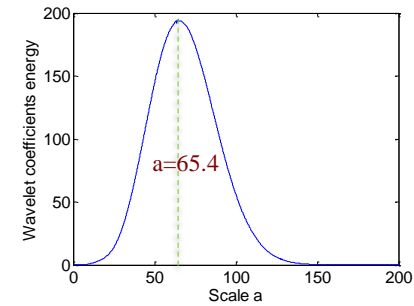


Vehicle properties		Bridge properties	
m_s	14000 kg	Span	15m
k_s	200 kN/m	Density	4800kg/m ³
c_s	10 kN s/m	Width	4 m
m_a	1000 kg	Depth	0.8m
k_a	2750 kN/m	Modulus	2.75×10^{10} N/m ²

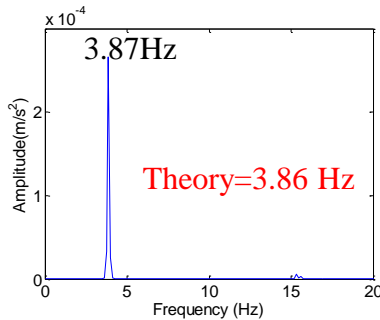
- Bridge frequency



$$E_{energy} = \sum_b^N |WT(a, b)|^2$$



Wavelet coefficient energy distribution



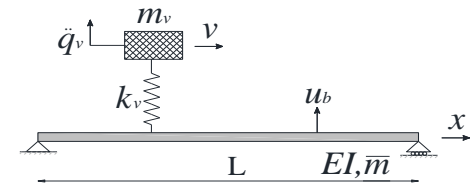
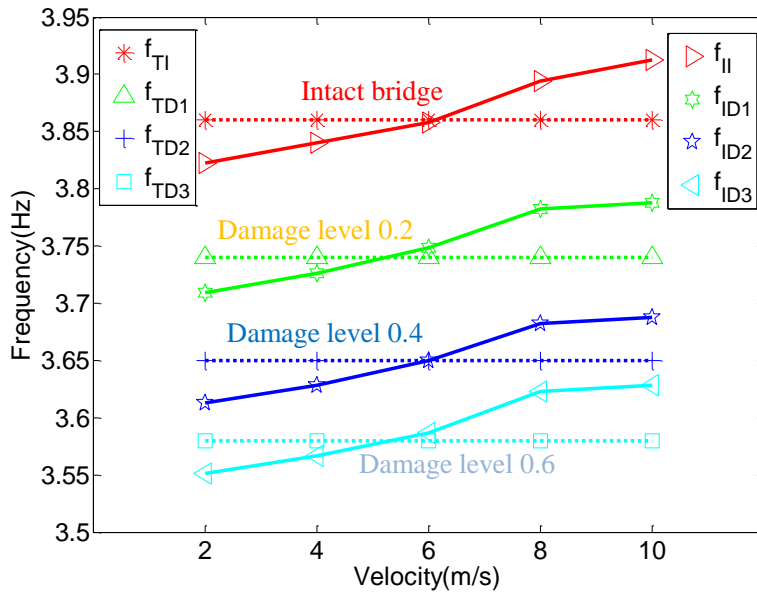
pseudo-frequency $F_S = \frac{F_C}{a\Delta}$

F_C is the **central frequency of the wavelet** in Hz (in this case, is :0.25Hz). a is the scale of the wavelet, and Δ is the **sampling period** of the signal (1000Hz).

$$F_S = \frac{0.25}{0.001 * 65.4} = 3.823$$

No resolution limitation

- Bridge damage detection



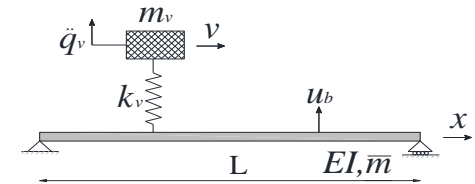
$$\ddot{q}_v(t) = \sum_{n=1}^{\infty} \left\{ \begin{aligned} &\bar{A}_{1,n} \cos\left(\frac{(n-1)\pi v}{L}\right)t + \bar{A}_{2,n} \cos\left(\frac{(n+1)\pi v}{L}\right)t + \bar{A}_{3,n} \cos(\omega_b t) \\ &+ \bar{A}_{4,n} \cos\left(\omega_{b,n} - \frac{n\pi v}{L}\right)t + \bar{A}_{5,n} \cos\left(\omega_{b,n} + \frac{n\pi v}{L}\right)t \end{aligned} \right\}$$

Shift frequency

The pseudo-frequency can detect the change of frequency, but the vehicle speed affects the identified frequency accuracy as well.

• Damping effect

Most of time, the bridge damping ratio is ignored for simplifying the vehicle response



$$\bar{m}\ddot{u} + EIu'''' = f_c(t)\delta(x - vt)$$

$$m_v\ddot{q}_v + k_v(q_v - u|_{x=vt}) = 0$$

Bridge motion equation:

Vehicle motion equation:

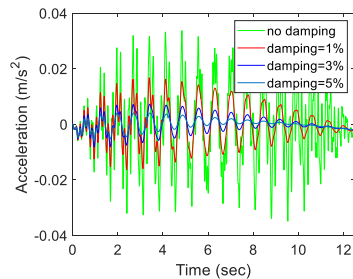
$$\bar{m}\ddot{u} + c_{b,e}\dot{u} + c_{b,i}I\dot{u}'''' + EIu'''' = f_c(t)\delta(x - vt)$$

$$m_v\ddot{q}_v + k_v(q_v - u|_{x=vt}) = 0$$

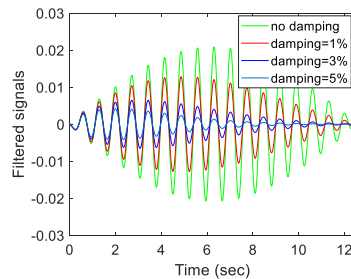
$$\ddot{q}_v(t) = \sum_{n=1}^{\infty} \left\{ \begin{aligned} &\bar{A}_{1,n} \cos\left(\frac{(n-1)\pi v}{L}t\right) + \bar{A}_{2,n} \cos\left(\frac{(n+1)\pi v}{L}t\right) + \bar{A}_{3,n} \cos(\omega_b t) \\ &+ \bar{A}_{4,n} \cos\left(\omega_{b,n} - \frac{n\pi v}{L}t\right) + \bar{A}_{5,n} \cos\left(\omega_{b,n} + \frac{n\pi v}{L}t\right) \end{aligned} \right\}$$

$$\begin{aligned} &\ddot{q}_v(t) \\ &= \sum_n \frac{\Delta_{st,n}}{2\sqrt{(1-S_n^2)^2 + 4S_n^2\varepsilon_{b,n}^2}} \left\{ \bar{A}_{1,n} \cos\left(\frac{2n\pi vt}{L} - \alpha\right) + \bar{A}_{2,n} \cos(\omega_v t + \alpha) \right. \\ &+ \bar{A}_{3,n} \cos(\omega_v t - \alpha) \\ &+ e^{-\varepsilon_{b,n}\omega_{b,n}t} \left[\bar{A}_{4,n} \cos(\omega_v t + \beta) + \bar{A}_{5,n} \sin(\omega_v t + \beta) + \bar{A}_{6,n} \cos\left(\omega_{b,n}t + \frac{n\pi vt}{L} - \beta\right) \right. \\ &+ \left. \bar{A}_{7,n} \cos\left(\omega_{b,n}t - \frac{n\pi vt}{L} - \beta\right) + \bar{A}_{8,n} \sin(\omega_{b,n}t + n\pi vt/L - \beta) \right] \end{aligned}$$

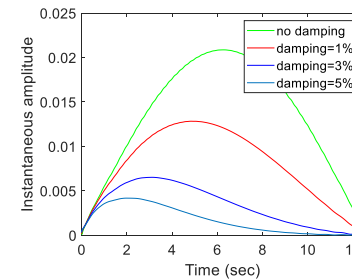
Yang etc. (2014) developed a Hilbert Transform based algorithm to extract mode shape from vehicle acceleration. They didn't consider the bridge damping, so they obtained: $HT\left(\frac{x}{v}\right) = constant \cdot \left|\sin\left(\frac{n\pi x}{L}\right)\right|$; if the damping exists, the formula changes to as $HT\left(\frac{x}{v}\right) = constant \cdot e^{-\varepsilon\omega(x/L)} \cdot \left|\sin\left(\frac{n\pi x}{L}\right)\right|$



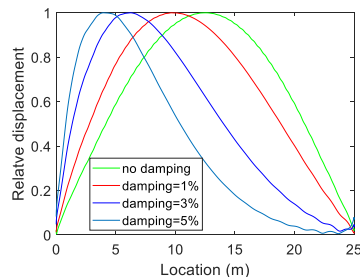
Vehicle acceleration



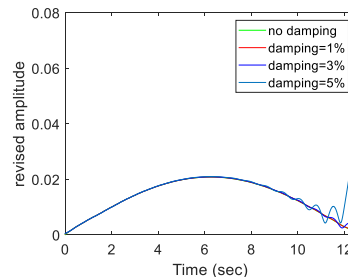
Filtered signals



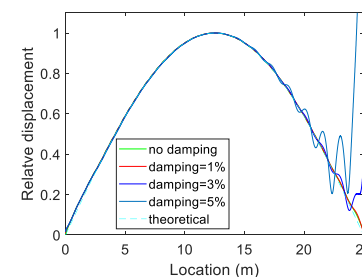
Amplitudes of HT



Yang's extracted mode shape



Revised amplitudes



Extracted mode shapes

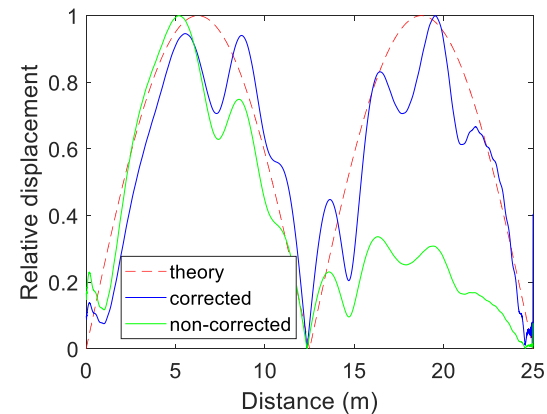
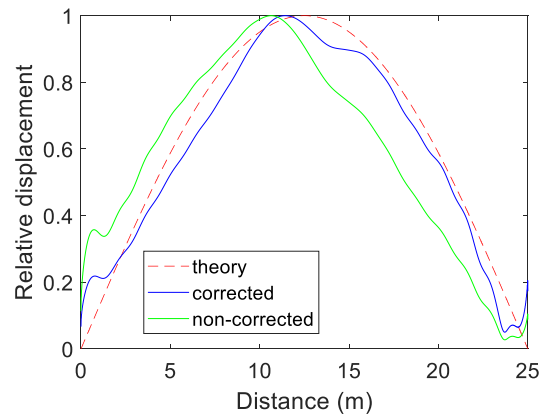
- Different vehicle speeds

Extracted damping for different vehicle speeds

Speed (m/s)	2	4	6	8	10
Damping ratio	0.0100	0.0100	0.0105	0.0160	0.0225
MAC	0.9998	0.9989	0.9968	0.9939	0.9914

High vehicle speed negatively affects the accuracy in both damping and mode shape.

- The effect of road roughness



Since the road roughness emerges a wide range of spatial frequency into the vehicle acceleration, the road roughness effect cannot be removed completely from the extracted mode shapes, using the frequency-domain filtering technique. In addition, the **extracted higher modes are easier to mingle with the road roughness, because of their lower amplitudes of higher modes comparing to those of lower.**

- Damage indexes

A scaling factor α is introduced, representing the minimum distance between the damaged and undamaged mode shapes

$$\alpha = \frac{MOSS_n^d \cdot MOSS_n^u}{MOSS_n^d \cdot MOSS_n^d}$$

where $MOSS_n^d$ and $MOSS_n^u$ are the n^{th} MOSS values of the damaged and undamaged structures, respectively. Then the damage index is defined by calculating the discrepancy between the MOSS values of damaged and undamaged bridges as

$$\Delta_n = MOSS_n^u - \alpha MOSS_n^d$$

When the damage location is not required, another damage indicator based on the **sum of differences between the MOSSs for the damaged and undamaged bridges** is

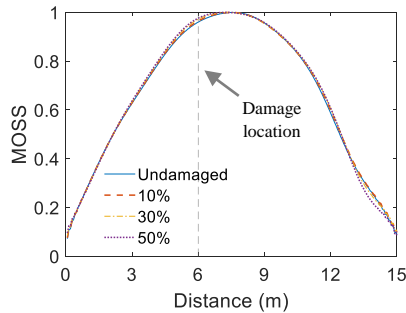
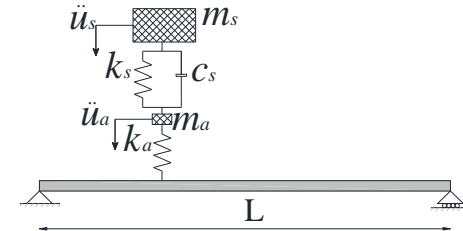
$$DI_n^* = \frac{1}{n_{ss}} \sum_{j=1}^{n_{ss}} |MOSS_n^u(j) - \alpha MOSS_n^d(j)|$$

- The procedural steps can be summarized as follows :

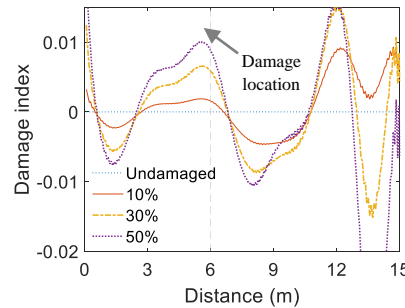
- (1) Acquire the bridge frequency $\omega_{b,n}$ and damping ratio $\varepsilon_{b,n}$. In practice, they can be obtained from a current or previous simple vibration experiment, or design values.
- (2) Calculate the corresponding instantaneous amplitudes, $A_n(t)$, with the target bridge natural frequency.
- (3) Reformulate the amplitude history with $A_n(t)/e^{-\varepsilon_{b,n}\omega_{b,n}t}$, and then normalize it to output MOSS.
- (4) Compare the output MOSS to that of the undamaged bridge and calculate the damage index.

- Numerical simulation

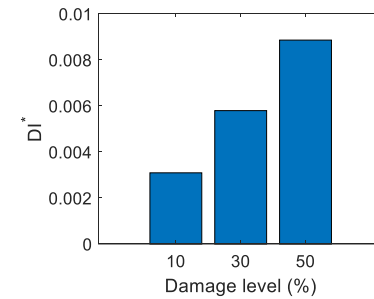
Vehicle properties		Bridge properties	
m_s	14300 kg	Span	15 m
k_s	200 kN/m	Density	4800 kg/m ³
c_s	10 kNs/m	Width	4 m
m_a	700 kg	Depth	0.8 m
k_a	2750 kN/m	Modulus	2.75×10 ¹⁰ N/m ²
		Damping ratio	0.02



Extracted MOSS for different damage levels



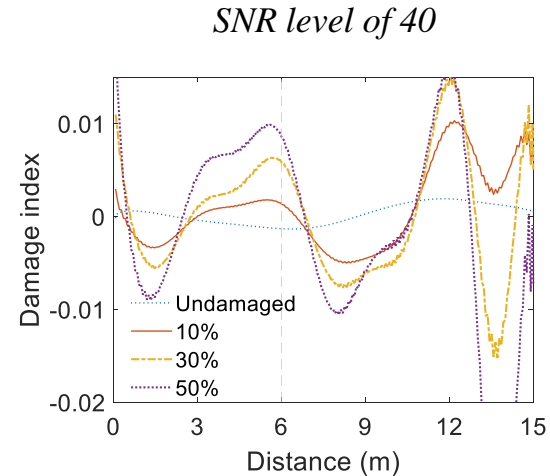
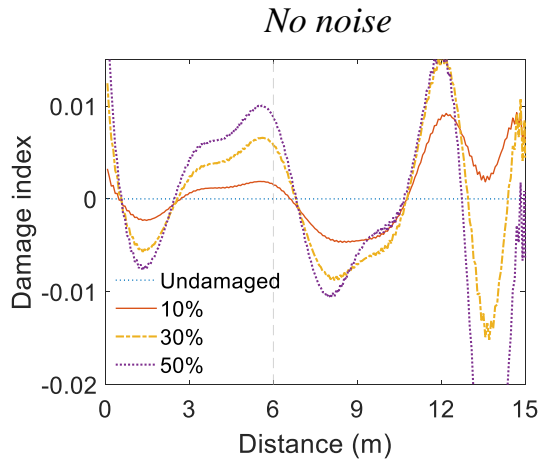
Damage index



Damage index DI* at different damage levels

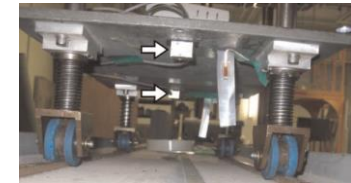
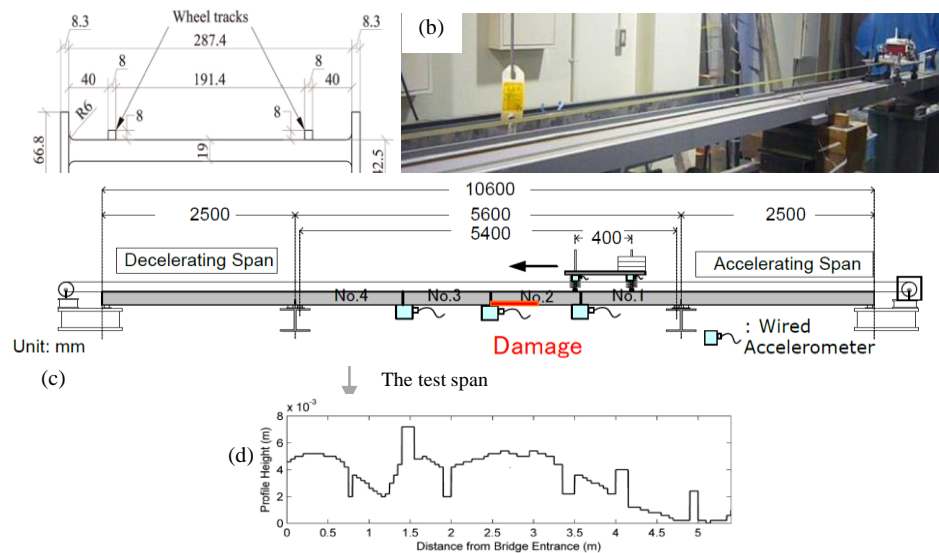
A peak close to the damage location can be seen when the damage level is 30% or more. The results demonstrate the ability of the algorithm to detect and, to some extent, localize damage. It is clear that DI* is well-correlated with the level of damage.

■ The effect of noise



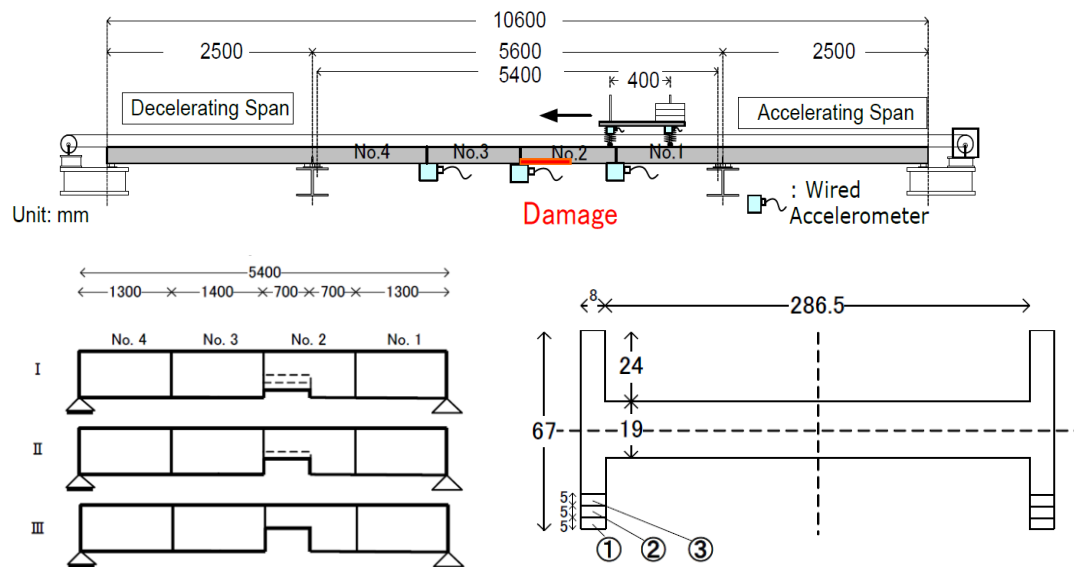
Here indicates that damage can still be detected from the index in the presence of noise. This is despite the fact that the band-pass filtering process in proposed algorithm reduces the impact of measurement noise, to some extent.

- Lab experiment—local damage



Intact case: (every speed runs 5 times)
 Scenario 1 – vehicle velocity is 0.93m/s.
 Scenario 2 – vehicle velocity is 1.16m/s.
 Scenario 3 – vehicle velocity is 1.63m/s.

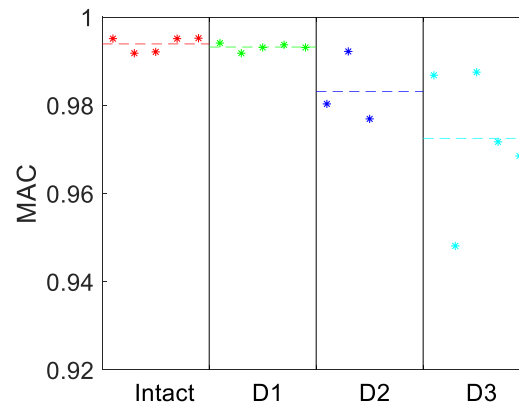
- Damage case of the lab experiment



Damage case (vehicle speed is 0.93 m/s)
 Scenario 1 – remove 5mm flange from the beam.
 Scenario 2 – remove 10mm flange from the beam.
 Scenario 3 – remove 15mm flange from the beam.

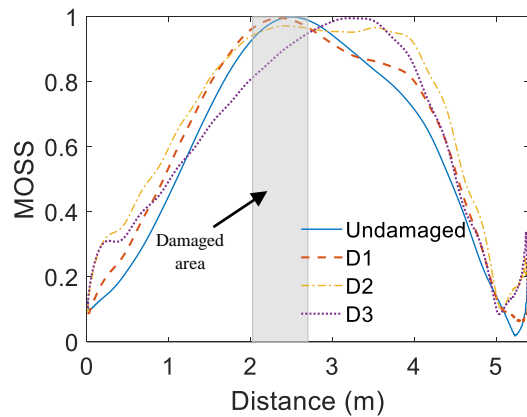
- Damage case results

It is clear that, as the damage level increases, the average MAC values decrease.

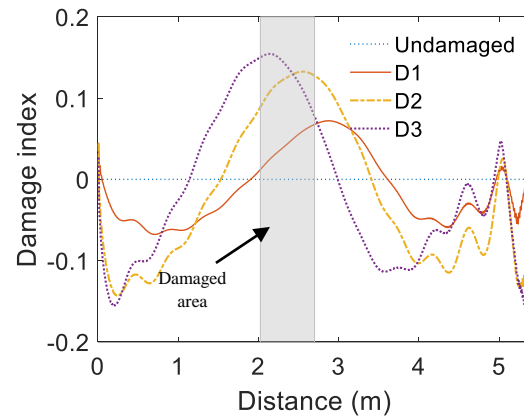


MAC values for different bridge conditions. Note: the dashed line represents the average value of five runs;

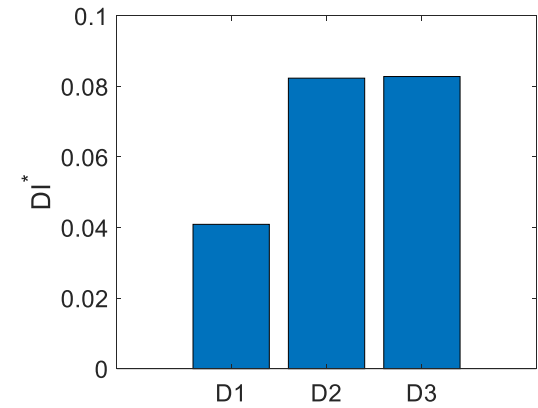
- Average results



Average extracted MOSS



Damage index DI



Damage index DI*

The damage index tends to increase with increasing damage and may also give an indication of damage location

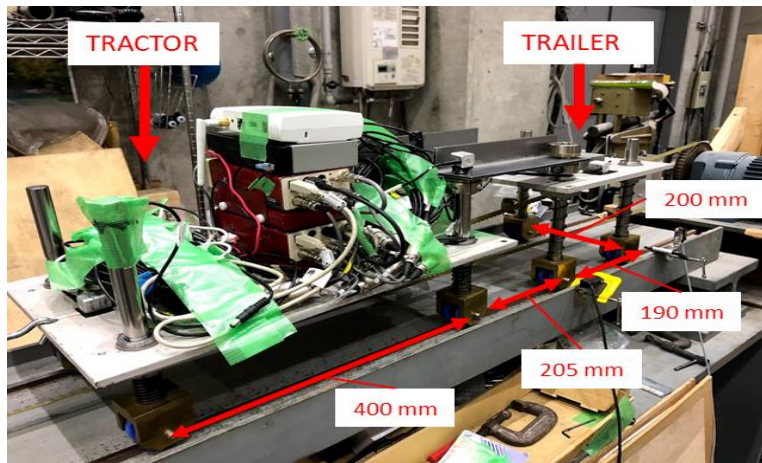
- Lab experiment—global damage



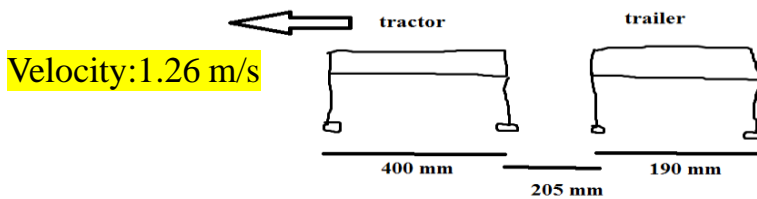
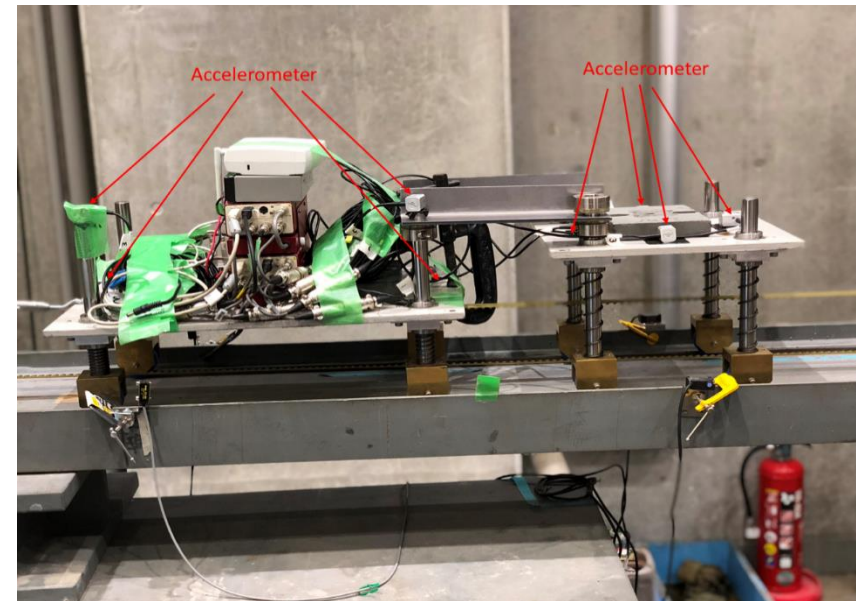
Span Length	1.3 m
Young's Modulus	$2.05 \times 10^{11} \text{ N/m}^2$
Density	$7.85 \times 10^3 \text{ kg/m}^3$
Beam depth	8.07 mm
Beam width	300 mm

The model bridge had four simply supported spans with the three internal piers supported on springs to represent the vertical stiffness provided by pad foundations; and scour is modelled as a reduction in stiffness due to scour .

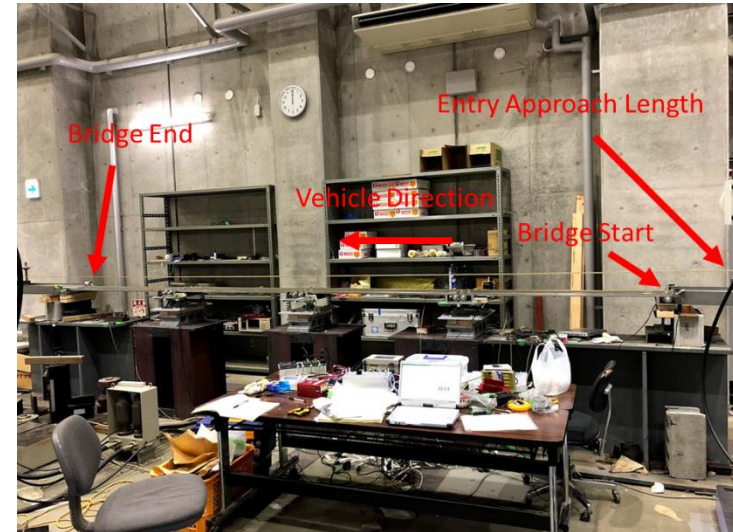
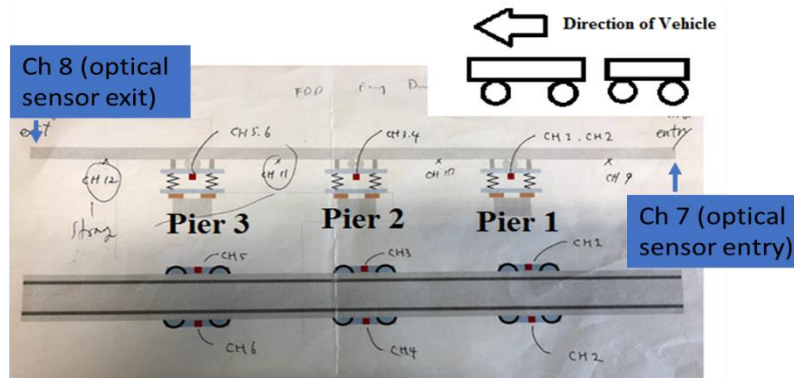
- Lab experiment—global damage—instrumented vehicles



	Weight	Unit
Tractor Front Axle	11.1	kg
Tractor Rear Axle	14.2	kg
Trailer Front Axle	6.7	kg
Trailer Rear Axle	7	kg

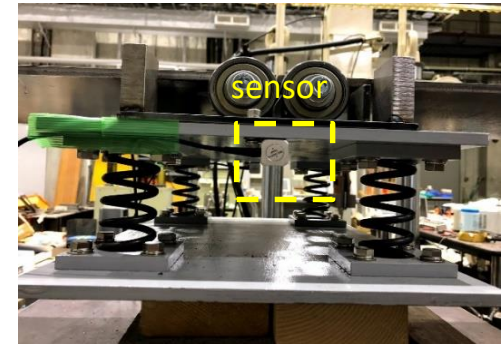
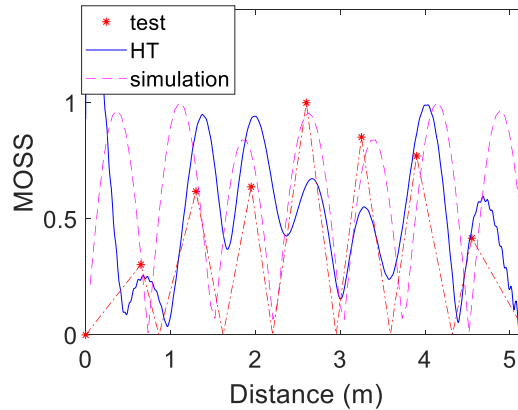
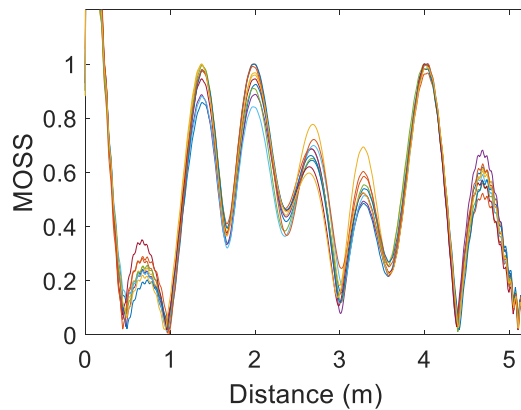


- Lab experiment—global damage scenarios



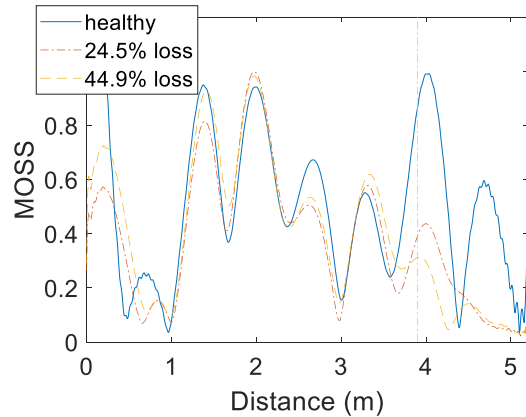
- A vehicle crosses a four span bridge multiple times. The piers are supported on springs and scour is modelled as a reduction in stiffness due to scour. For this, four weaker springs replaced the existing healthy springs.
- Five scour scenarios are investigated – [Healthy](#), 24.5% stiffness loss Pier 2, 44.9% stiffness loss Pier 2, 44.9% stiffness loss Pier 3, 24.5% stiffness loss Pier 3.
- Each “healthy” spring had a stiffness of 49 N/mm, which was determined from load-displacement tests. As 4 springs were used under each pier, the combined vertical stiffness is 196 N/mm.

- Bridge mode shape extraction

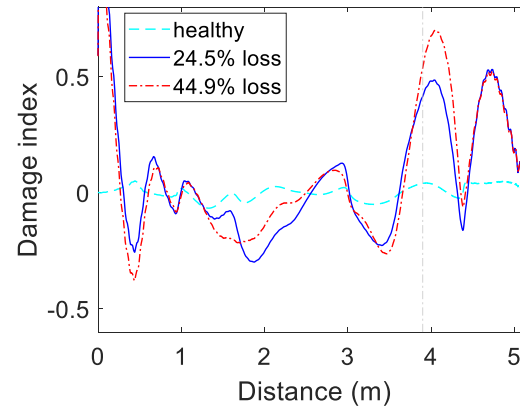


It is found that in this case, this approach only performs excellently on extracting the 5th bridge mode shape, since the extracted results shows well repeatability for repeat runs with bridge frequency of 21.9 Hz. For other bridge frequencies, there is no apparent repeatability of the extracted results for repeat runs

- Global damage detection-Pier 3



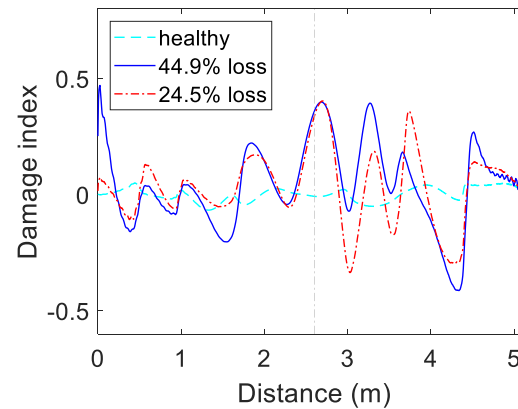
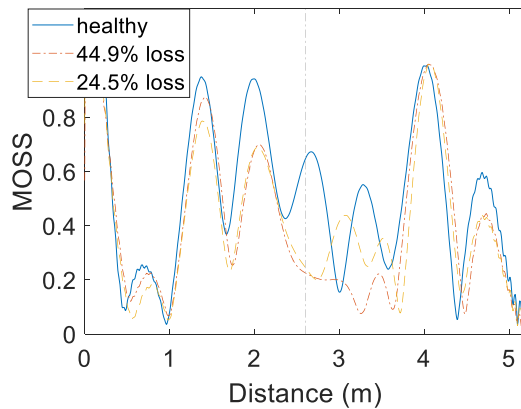
Experimental result with damage at pier 3



Damage index with pier 3

Another damage index DI^* is calculated as well (undamaged=0.0309; 24.5% loss=0.1986; 44.9 % loss=0.2086)

- Global damage detection-Pier 2



The damage index can show a great difference between healthy and damage bridge conditions as well. The damage index DI^* is also calculated for this case (healthy=0.0310; 24.5% loss=0.1209; 44.9 % loss=0.1456).

Journal Publications

1. Tan, C., Elhatab, A., and Uddin, N. (2020) "Wavelet-Entropy Approach for Detection of Bridge Damages using Direct and Indirect Bridge Records"; *Journal of Infrastructure Systems* Volume 26 Issue 4 - December 2020
2. Yahya M M, Nasim U, Chenjun T, Zhenhua S. (2020) "Crack Detection using Faster R-CNN and Point Feature Matching". *Civil Eng Res J.* 2020; 10(3): 555790.DOI: 10.19080/CERJ.2020.10.555790.
3. Tan, C. and Uddin, N. (2020) "Hilbert transform based approach to improve extraction of "drive-by" bridge frequency", *Smart Structures and Systems* Volume 25, Number 3, March 2020, pages 265-277; DOI: <https://doi.org/10.12989/sss.2020.25.3.265>
4. Tan, Chengjun, Uddin, N., Eugene J. OBrien, Patrick J McGetrick, and Chul-Woo Kim (2020). "Extracting Mode Shapes from Drive-By Measurements to Detect Global and Local Damage in Bridges." *Structure and Infrastructure Engineering* (accepted for publication)
5. Tan, C. and Uddin, N. (2020) "Structural Health Monitoring of Bridges – the Conflicting Challenges of Detecting Global and Local Damage", *Structure and Infrastructure Engineering* (accepted for publication)
6. Elhatab, A., Uddin, N., and OBrien, E., (2019) "Extraction of Bridge Fundamental Frequencies Utilizing a Smartphone MEMS Accelerometer"; *Journal Sensors*; 2019, 19(14), 3143; <https://doi.org/10.3390/s19143143>
7. Tan, Chengjun, Uddin, N., Eugene J. OBrien, Patrick J McGetrick, and Chul-Woo Kim (2019). "Extraction of Bridge Modal Parameters Using a Passing Vehicle Response." *Journal of Bridge Engineering* (ASCE); Volume 24 Issue 9 - September 2019
8. Mohammed, Y., and Uddin, N. (2019) "Acceleration-Based Bridge Weigh-in-Motion"; *Journal of Bridge Structures* 14(4): 131-138.
9. Mohammed, Y., and Uddin, N. (2019) "Moving Force Identification for Real-Time Bridge Weigh-In-Motion"; *Journal of Bridge Structures*; 14(4): 139-145.
10. Mohammed, Y., and Uddin, N. "B-WIM System using Fewer Sensor", *J. Transportation Management* (2018) Volume 1, Issue 2, doi:10.24294/tm.v1i2.701
11. Elhatab, A., Uddin, N., and OBrien, E., (2018) "Drive-By Bridge Frequency Identification under Operational Roadway Speeds Employing Frequency Independent Underdamped Pinning Stochastic Resonance (FI-UPSR)"; *Journal Sensors*; 2018, 18(12), 4207; <https://doi.org/10.3390/s18124207>
12. Tan, C. and Uddin, N. (2017) "Drive-By" Bridge Frequency Based Monitoring Utilizing Wavelet Transform", *Journal of Civil Structural Health Monitoring*, November 2017, Volume 7, Issue 5, pp 615–62
13. Elhatab A. and Uddin, N. (2017) "Drive-by Bridge Damage Monitoring: Concise Review", *Civil Eng Res Journal, CERJ*.MS.ID.555555 (2017), Volume 1 Issue 1 - July 2017
14. Lydon, M., Robinson, D., Taylor, S., Amato, G., Brien, E. J. O. & Uddin, N. "Improved Axle Detection for Bridge Weigh-In-Motion System using Fiber Optic Sensors", 12 Jul 2017, [Journal of Civil Structural Health Monitoring](#), 7, 3, p. 325-332
15. Elhatab A. and Uddin, N. (2017) "Drive-by Bridge Damage Detection Using Non-Specialized instrumented vehicle", *Journal of Bridge Structures*, accepted for publication.
16. Elhatab, A., Uddin, N., and OBrien, E., 2016, "Drive-by bridge damage monitoring using Bridge Displacement Profile Difference," *Journal of Civil Structural Health Monitoring*, 6(5), pp. 839-850.
17. Kalyankar, R., and Uddin, N. (2017) "Axle Detection on Prestressed Concrete Bridge Using Bridge Weigh-In-Motion System", *Journal of Civil Structural Health Monitoring*, accepted for publication.
18. Zhao, Z. and Uddin, N. (2017) "Bridge Weigh-in-Motion Algorithms Based on the Field Calibrated Simulation Model" *ASCE Journal of Infrastructure System*, February 2016, *Journal of Infrastructure Systems*, Volume 23 Issue 1 - March 2017
19. Kalyankar, R. R., and Uddin, N. (2017), "Simulation of Advanced 3D Finite Element Dynamic Vehicle Bridge Interaction Using Single and Multi-Vehicle Scenario for Obtaining Dynamic Amplification Factor," *Int. Journal of Bridge Engineering*, Volume 5, Issue 2 (May. - Aug. 2017).
20. Kalyankar, R. R., and Uddin, N. (2016), "Simulating the Effects of Surface Roughness on Reinforced Concrete T Beam Bridge under Single and Multiple Vehicles," *Advances in Acoustics and Vibration*, vol. 2016, Article ID 3594148, 12 pages, 2016. doi:10.1155/2016/3594148.
21. Pandey, S., Haider, M. and Uddin, N. (2016) "Design and Implementation of a Low-Cost Wireless Platform for Remote Bridge Health Monitoring", *International Journal of Emerging Technology and Advanced Engineering*, Volume 6, Issue 6, June 2016
22. Lydon, M., Robinson, D., Taylor, S. E., OBrien, E., Uddin, N. (2016) "Next generation bridge weigh-in-motion system: optimized using explicit finite element analysis" *ASCE Journal of Bridge Engineering*, Accepted for publication.
23. Zhao, H. and Uddin, N. (2014) "Field-Calibrated Algorithm to Identify Axle Weights for BWIM Systems"; *Structure and Infrastructure Engineering*, *Structure and Infrastructure Engineering*, Vol. 11, No. 6, June 2015, pp. 721-743.
24. Zhao, H. and Uddin, N. (2014) "Identification of Vehicular Axle Weights with a BWIM System Considering Transverse Distribution of Wheel Loads"; *ASCE Journal of Bridge Engineering*, Vol. 19, Issue 3, 2014.
25. Zhao, Z. and Uddin, N. (2013) "Determination of Dynamic Amplification Factors Using Site-Specific B-WIM Data" *ASCE Journal of Bridge Engineering*, Vol. 19, No. 1, January 1, 2014.
26. Zhao, Z. and Uddin, N. (2013) "Field Calibrated Simulation Model to Perform Bridge Safety Analyses against Extreme Events", *Journal of Engineering Structures*, 56 (2013) 2253–2262.

Summary and Conclusion

Results:

Current bottlenecks in the areas of challenges of continuous power supply, generating large volume of data, and lack of understanding of bridge load and performance have been addressed by innovative fly-by and drive-by monitoring system:

- Fly-by monitoring using drone has demonstrated significant potential to complement bridge inspection
- Prototype development of drone charging pads and fly-by drone sensors is a major step forward
- Different types of drone sensing can be used based on required efficiency, quality of camera and available processors.
- Algorithms for bridge weigh-in-motion, damage detection on the fly, deformation monitoring and vibration sensing by hovering drones demonstrated reasonable success
- Drive-by monitoring and damage detection proved to be complementary system for the bridge inspection and management.

Discussions:

- More field testing will be pursued.
- Different type of stronger processor will be used.